Available online at www.sciencedirect.com

SciVerse ScienceDirect

Geochimica et Cosmochimica Acta 112 (2013) 305–320

Geochimica et Cosmochimica Acta

www.elsevier.com/locate/gca

Co-variation of nitrogen isotopes and redox states through glacial–interglacial cycles in the Black Sea

Tracy M. Quan [a,*], James D. Wright [b], Paul G. Falkowski [a,b]

[a] Institute of Marine and Coastal Sciences, Rutgers University, 71 Dudley Road, New Brunswick, NJ 08901, United States
[b] Department of Earth and Planetary Sciences, Rutgers University, 610 Taylor Road, Piscataway, NJ 08854, United States

Received 18 January 2012; accepted in revised form 25 February 2013; Available online 7 March 2013

Abstract

In all aquatic environments, nitrogen cycling within the water column is strongly influenced by oxygen. We hypothesize that the nitrogen isotopic composition ($\delta^{15}N$) of organic matter deposited in the sediments is a proxy for the redox state of the water column at the time of deposition. We tested the hypothesis by measuring the bulk sedimentary $\delta^{15}N$ values in a drill core from the Black Sea, a basin that alternates between oxic, less saline conditions and anoxic, marine conditions on glacial–interglacial time scales. We reconstructed these changes in Black Sea redox conditions using sedimentary $\delta^{15}N$, total organic carbon (TOC), total nitrogen (TN), redox-sensitive metals, and micropaleontological data from a deep-sea core (DSDP Site 380). The sedimentary data reveal that during the transitions between oxic and anoxic conditions, $\delta^{15}N$ values increased relative to the preceding and succeeding quasi-steady-state oxic and anoxic periods. The results indicate that the reciprocal transitional states from anoxic to oxic conditions were accompanied by intense denitrification; during the quasi-stable oxic and anoxic states (characterized by glacial fresh water and interglacial marine conditions) nitrification and complete nitrate utilization, respectively, dominate the nitrogen cycle. While other factors may influence the $\delta^{15}N$ record, our results support the hypothesis that the variations in nitrogen isotopic composition of organic matter are strongly influenced by changes in redox state in the Black Sea subphotic zone on glacial–interglacial time scales, and can be explained by a relatively simple model describing the effects of oxygen on the microbial processes that drive the nitrogen cycle in marine ecosystems. Our model suggests that the nitrogen isotopic composition of marine sediments, on geological time scales, can be used to reconstruct the redox state of the overlying water column.

1. INTRODUCTION

Nitrogen is an essential macronutrient for growth and effective trophic transfer in all ecosystems. In aquatic ecosystems, the availability of fixed inorganic nitrogen is strongly influenced by the redox state of the water column below the euphotic zone (Quan and Falkowski, 2009). The backbone of the nitrogen cycle consists of three main processes: nitrogen fixation, nitrification, and denitrification/anammox (since denitrification and anammox appear to occur under similar environmental conditions and are assumed to have similar isotopic fractionations, we will refer to both reactions simply as "denitrification"). These three reactions form a circuit of coupled reduction/oxidation/reduction reactions, which are alternately sensitive to, or dependent upon, oxygen (Falkowski, 1997; Fennel et al., 2005). While other reactions can influence nitrogen cycling on seasonal to decadal time scales, the balance between nitrogen input via fixation and removal through denitrification controls the pool of fixed inorganic nitrogen in aquatic ecosystems on millennial time scales and strongly influences oxygen and carbon cycles (Falkowski, 1997; Jenkyns et al., 2001, 2007; Fennel et al., 2005; Moore and Doney, 2007; Falkowski and Godfrey, 2008).

* Corresponding author. Present address: Boone Pickens School of Geology, Oklahoma State University, 105 Noble Research Center, Stillwater, OK 74078, United States.
E-mail address: tracy.quan@okstate.edu (T.M. Quan).

0016-7037/$ - see front matter © 2013 Elsevier Ltd. All rights reserved.
http://dx.doi.org/10.1016/j.gca.2013.02.029

The isotopic composition of well-preserved sedimentary organic compounds can serve as reliable indicators of water column nitrogen reactions (e.g. Altabet and Francois, 1994; Ganeshram et al., 1995, 2000, 2002; Calvert et al., 2001; Jenkyns et al., 2001, 2002, 2007; Kienast et al., 2002). By correlating sedimentary $\delta^{15}N$ values with changes in water column redox state for a particular site, several characteristics about the water column, including primary productivity, deep water N:P ratios, and carbon burial can be inferred (e.g. Ganeshram et al., 1995, 2000, 2002; Kienast et al., 2002; Quan and Falkowski, 2009; Sigman et al., 2009).

Previously, we demonstrated that the nitrogen isotopic composition in the sediments was related to deep water O_2 concentrations and thus water column redox state, following a simple, non-linear curve as outlined in Quan et al. (2008) (Fig. 1A). The non-linear relationship is based on the redox coupling of the three basic reactions that govern nitrogen cycling in the water column on millennial scales. The relative intensity of each of the reactions can be inferred from nitrogen isotopic signatures of organic matter that is exported to the sediments, therefore allowing bulk sediment (as well as any compound-specific fractions isolated from the sediment) to serve as proxies for the water column nitrogen cycle. Incomplete denitrification is characterized by a strong, positive fractionation that results in the residual nitrate pool becoming enriched in ^{15}N, which is subsequently utilized by autotrophs to produce organic matter enriched in ^{15}N. Similarly, sedimentary $\delta^{15}N$ values in predominantly nitrogen fixing or nitrifying systems have lower $\delta^{15}N$ due to the smaller, less positive fractionation factors for these processes. Under anoxic conditions, nitrification is minimal and hence the amount of denitrification is lower; the concordant isotopic values of organic N are close to that of nitrogen fixation. As the amount of oxygen in the system increases, both nitrification and denitrification become increasingly predominant, and the $\delta^{15}N$ of the organic matter produced and buried in the sediment rises accordingly. At fully oxygenated levels, the denitrification reactions are inhibited, and other nitrogen reactions (nitrification, nitrogen assimilation, and nitrogen fixation) with smaller fractionation factors predominate. Using this conceptual model, a significant positive shift in a measured $\delta^{15}N$ record indicates a suboxic water column. It should be noted that because the model is non-linear, identical $\delta^{15}N$ values can exist at two different oxygen concentrations (Fig. 1A). Thus, to constrain the interpretation of $\delta^{15}N$ in the sedimentary record, an independent measure of redox should also be obtained (Quan et al., 2008).

Sedimentary $\delta^{15}N$ data from a variety of redox environments are necessary to validate this model. We previously demonstrated that higher $\delta^{15}N$ values were associated with enrichments in redox-sensitive elements and thus lower water column oxygen concentrations in coastal sediments deposited in the Tethys Sea across the Triassic–Jurassic boundary (Quan et al., 2008). Nitrogen isotopic records have been reported across a spectrum of geological settings and time periods where distinct changes in oxidation state have been suspected, such as modern-day suboxic/anoxic waters (e.g. Thunell et al., 2004; Gaye-Haake et al., 2005; Naqvi et al., 2006; Cowie et al., 2009; Sigman et al., 2009; Ward et al., 2009; Ryabenko et al., 2012), oceanic anoxic events (e.g. Jenkyns et al., 2001, 2007; Dumitrescu and Brassell, 2006; Juniam and Arthur, 2007) or glacial–interglacial cycling in continental margins and restricted basins (e.g. Ganeshram et al., 1995; Haug et al., 1998; Pride et al., 1999; Emmer and Thunell, 2000; Ganeshram et al., 2000, 2002; Thunell and Kepple, 2004). The $\delta^{15}N$ records from these environments allow qualitative changes in environmental redox conditions to be inferred: intervals of higher $\delta^{15}N$ values imply increased net denitrification, suboxic oxygen concentrations, and expanded oxygen minimum zones (OMZ), while periods of lower $\delta^{15}N$ values are presumably indicative of conditions favorable to increased net nitrogen fixation, a decrease in OMZ volume, or periods in which denitrification has gone to completion. While important for evaluating paleo-nitrogen cycling, these studies are often limited by the short time interval sampled, small basin sizes, unknown degree of environmental redox change, and/or relatively low sedimentation rates. It is critical that nitrogen cycle dynamics (and the resulting $\delta^{15}N$ signals) under varying environmental and redox conditions be investigated and understood in order to have a foundation for interpreting sedimentary $\delta^{15}N$ records through deep time events.

With this goal in mind, the Black Sea would appear to be an ideal study site to test our model of $\delta^{15}N$ variability with changes in redox state due to the intensity and pattern of the redox shifts in the basin. The Black Sea redox state has varied between oxic to anoxic over the most recent glacial to interglacial cycle (e.g. Ross and Degens, 1974; Olteanu, 1978; Ross, 1978; Hsü, 1978a; Major et al., 2002; Lüschen, 2004; Neretin et al., 2004; Nagler et al., 2005). During the last glacial interval, the enclosed basin is usually considered to be fully oxic, in contrast to the completely anoxic bottom waters observed during interglacial periods (e.g. Ross and Degens, 1974; Schrader, 1979; Aksu et al., 2002). A conceptual model of the water column structure with respect to nitrogen under oxic, anoxic, and transitional redox conditions in the Black Sea is presented in Fig. 1B. By combining the water column model with the model linking sedimentary $\delta^{15}N$ values to bottom water oxygen concentrations (Fig. 1A), we can predict the sedimentary $\delta^{15}N$ response to glacial–interglacial redox changes in the basin (Fig. 1C).

In this paper we report the bulk sedimentary $\delta^{15}N$ results from Deep Sea Drilling Project (DSDP) Site 380, drilled in the Black Sea. In addition to the $\delta^{15}N$ measurements, we also measured a range of geochemical and micropaleontological proxies to constrain the redox state of the water column in the Black Sea, and thus the main processes controlling the $\delta^{15}N$ record. The paleoredox proxies are compared with the $\delta^{15}N$ record to test the predictions by our conceptual model concerning $\delta^{15}N$ values versus O_2.

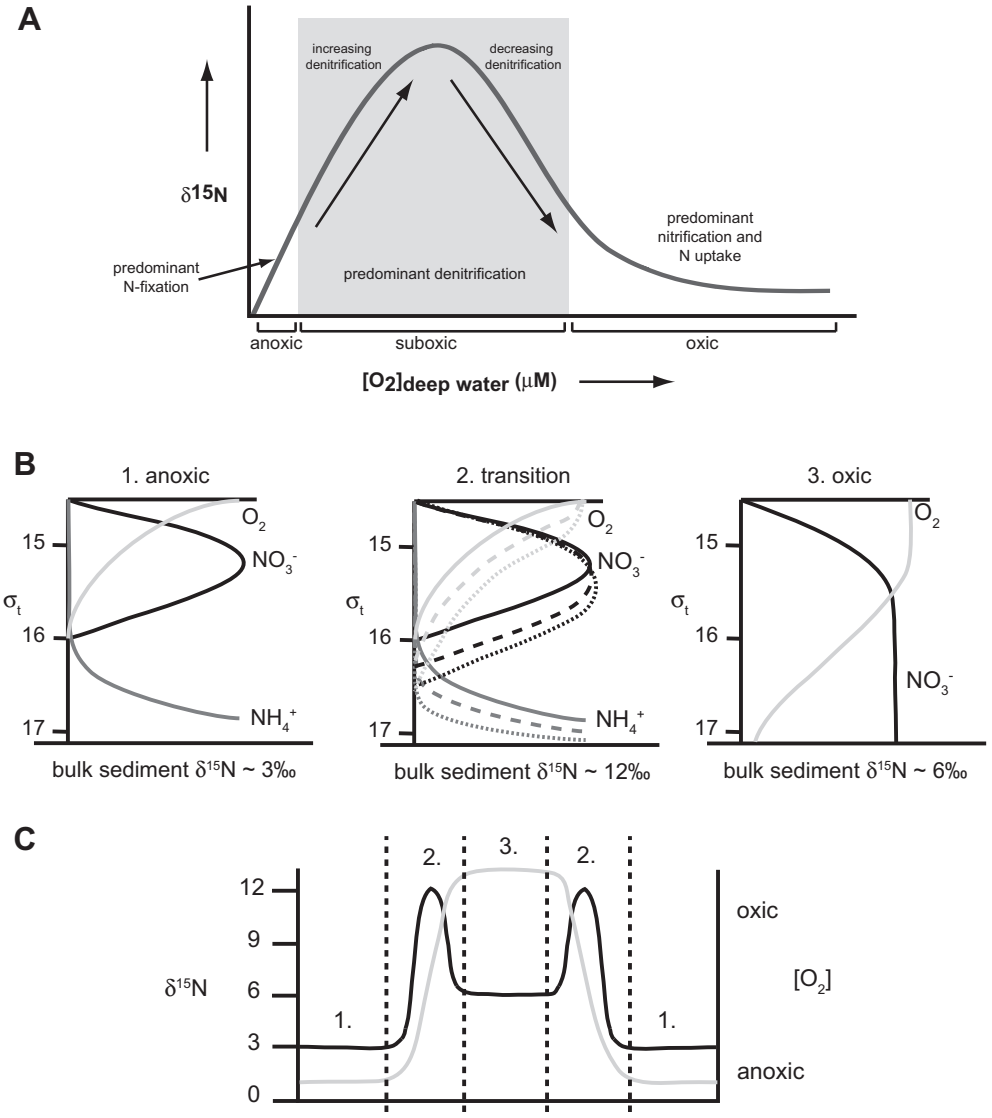

Fig. 1. Part A illustrates the conceptual model of how sedimentary $\delta^{15}N$ values correlate to changes in deep water oxygen levels (adapted from Quan et al., 2008). Enriched $\delta^{15}N$ values resulting from predominant water column denitrification are found within the shaded suboxic zone. Part B consists of a series of idealized water column profiles for O_2 (light gray), NO_3^- (black), and NH_4^+ (dark gray) for the Black Sea under three different redox regimes, along with the hypothesized surface sediment $\delta^{15}N$ values (profiles modeled after Kuypers et al. (2003) and Murray et al. (2005)). Scenario 1 represents anoxic conditions similar to the current interglacial. As the basin transitions to oxic conditions, the curves shift downwards in the water column (solid to dashed to dotted curves; scenario 2). Fully oxic glacial conditions are indicated in scenario 3. In part C, predicted sedimentary $\delta^{15}N$ values (black) change in concert with changes in O_2 (light gray) through one complete glacial–interglacial cycle.

2. SETTING, MATERIALS AND METHODS

2.1. Geological setting

The modern Black Sea is the largest anoxic basin in the contemporary ocean, and as such, it potentially serves as a proxy model of alternative biogeochemical reactions in the global ocean on geological time scales. The modern stratified basin is characterized by a shallow layer of oxic, nutrient-depleted water overlying anoxic, saline deep-waters. However, environmental and redox conditions of the basin appear to have changed drastically with the rise and fall of global sea levels (Ross and Degens, 1974; Aksu et al., 1999, 2002; Ryan et al., 2003; Major et al., 2006). Periods of high sea stand, such as during interglacial intervals, allow the exchange of surface waters between the Black Sea and Mediterranean Sea through the Bosphorus Straits and Marmara Sea. Freshwater flow to the basin is from the Danube and other rivers draining southern Europe and western Asia. The 50 m sill depth of the Bosphorus restricts deep water exchange between the Black and the Mediterranean Seas; the Black Sea deep water is a mix of surface inflow with ambient Black Sea water (Murray et al., 1991). This pattern of freshwater export from the Black Sea at the surface with

saline inflow underneath, along with the remineralization of organic matter, results in a highly stratified basin, with less dense, more oxic surface waters overlying a more saline, anoxic deep water, with a thin suboxic layer (generally located between 15.4 and 16.2 σ_t) between them (Nutrient profiles in the Black Sea have a stronger correlation with density than with depth, so layer boundaries are often given as densities, rather than in meters). When connected to the Mediterranean, conditions in the deep basin are reducing/anoxic due to the net estuarine circulation, resulting in sediments with generally higher organic matter content. Nitrate is low in the euphotic zone due to biological uptake, then increases to a maxima in the suboxic zone at ~100 m (~15.5 σ_t) (Codispoti et al., 1991; Murray et al., 1995, 2005; Kuypers et al., 2003; McCarthy et al., 2007; Fuchsman et al., 2008). Both denitrification and anammox reactions are known to occur in the modern-day Black Sea, and both appear to go to completion (Codispoti et al., 1991; Murray et al., 2005; Çoban-Yıldız et al., 2006). Below ~150 m (~16.2 σ_t), ammonia is the dominant form of dissolved inorganic nitrogen in the anoxic zone (Fig. 1A; Kuypers et al., 2003; Murray et al., 2005; McCarthy et al., 2007). The oxygen-rich Cold Intermediate Layer (CIL), serves as the main oxygen source for deeper waters in the Black Sea, and is marked by a temperature minimum at approximately 50–100 m (14.5 σ_t, which sits at the top of the pycnoline) (Konovalov et al., 2003, 2005; Murray et al., 2005). The CIL mixes with the marine water entering through the Bosphorus to form oxygen rich lateral intrusions (Özsoy et al., 1991, 2002; Konovalov et al., 2003, 2005; Gregg and Yakushev, 2005). Variations in the concentration and depth distribution of nitrogen species, as well as the thickness of the suboxic zone appear to occur on seasonal, yearly, and decadal time scales in the modern-day Black Sea, potentially driven by climatic and/or anthropogenic changes (Codispoti et al., 1991; Konovalov et al., 2005; Murray et al., 2005; Fuchsman et al., 2008).

In contrast, the marine connection to the Mediterranean Sea is severed during glacial periods by lower sea levels resulting in less saline, nearly freshwater lacustrine conditions (Fig. 1A). The sedimentary record of freshwater ostracods, trace metal profiles, radiocarbon reservoir age, the steppe-forest pollen climate index, and the deposition of *seekeride* (lake deposited chalk) imply that the water column was oxic and well mixed (Olteanu, 1978; Traverse, 1978; Hsü, 1978a; Major et al., 2002; Lüschen, 2004; Neretin et al., 2004; Nagler et al., 2005; Kwiecien et al., 2008). Changes in water column salinity and oxygenation state have been reconstructed using the micropaleontological groups present in the sediment samples. For example, the presence of coccoliths and planktonic foraminifera species (Hsü, 1978a; Calvert et al., 1987; Lyons, 1991; Aksu et al., 2002), and marine diatoms (Schrader, 1979) indicate marine waters were present as the Black Sea reconnected to the Mediterranean Sea (Ryan et al., 1997, 2003; Aksu et al., 1999, 2002). Fresh water environments are inferred from the presence of the ostracod *Candona,* which also indicates a homogenized water column immediately after the first marine inflows at the end of the glacial interval (Bahr et al., 2006, 2008; Major et al., 2006). Many of the benthic foraminifera present represent taxa with affinities towards brackish and hypoxic conditions (Gheorghian, 1974; Yanko-Hombach, 2007) suggesting some low level salinity at depth. Trace metal isotopic and concentration profiles also indicate a distinct change in redox conditions in the last glacial compared to the current interglacial (Arnold et al., 2004; Lüschen, 2004; Neretin et al., 2004; Nagler et al., 2005).

2.2. Sediment samples and preparation

Sediment samples from the Black Sea were taken from the DSDP Site 380, which is located in the southwest corner of the basin, just to the north of the Bosphorus Straits in a water depth of 2115 m (Fig. 2). Two holes were drilled at this site: Hole 380 drilled to a depth of 370.5 meters below sea floor (mbsf), and Hole 380A, washed down to where Hole 380 stopped and continued to a final depth of 1073 mbsf. The combined record extends from the Pleistocene into the Late Miocene (Hsü, 1978b; Popescu, 2006). The lithology is classified as predominantly terrigenous sediments, mainly mud with minor intercalations of sandy silts and silty clays (Ross, 1978).

Thirty-four samples were collected from the upper Pleistocene section of Site 380 from 0 to 118.31 mbsf. Care was taken to scrape off the sides and tops of the samples when possible to remove potential surface contamination; some of the samples were too sandy to do so. All samples were dried overnight at 35 °C. The sample was then split: approximately 2 g of each sample was crushed to a powder using a ceramic mortar and pestle for measurements of total organic carbon (TOC) and nitrogen (TN), trace element analysis, and carbon and nitrogen isotopic analyses; the remainder of the original sample was used for micropaleontological analyses.

2.3. Organic carbon and nitrogen concentration and stable isotope analyses

Measurements of both $\delta^{13}C_{org}$ and $\delta^{15}N$ were performed on a Eurovector elemental analyzer attached under continuous flow to a GV Instruments IsoPrime isotope ratio mass spectrometer, using procedures described previously (Quan et al., 2008). Samples for $\delta^{15}N$ were performed on bulk sediment; samples run for $\delta^{13}C_{org}$ were decarbonated in silver capsules using hydrochloric acid. Values for TN were calculated as the weight percent nitrogen in the bulk sediment; TOC values were calculated as the weight percent carbon in the decarbonated samples. Replicates of both samples and standards for $\delta^{13}C_{org}$ had a standard deviation of $<\pm 0.2‰$; the variation in TOC was <0.03%. Triplicate analyses of the Black Sea nitrogen samples had a standard deviation of less than $\pm 0.2‰$ for $\delta^{15}N$ and the variation in TN was <0.03%. Variation ($1-\sigma$) in the in-house standard mix was determined to be $\pm 0.2‰$ ($n = 42$).

2.4. Micropaleontological analyses

Each sample was washed through a 63 μm sieve. The remaining coarse fraction was examined for the presence/absence of planktonic and benthic foraminifera and ostracods. Taxonomic analyses of planktonic and benthic foram-

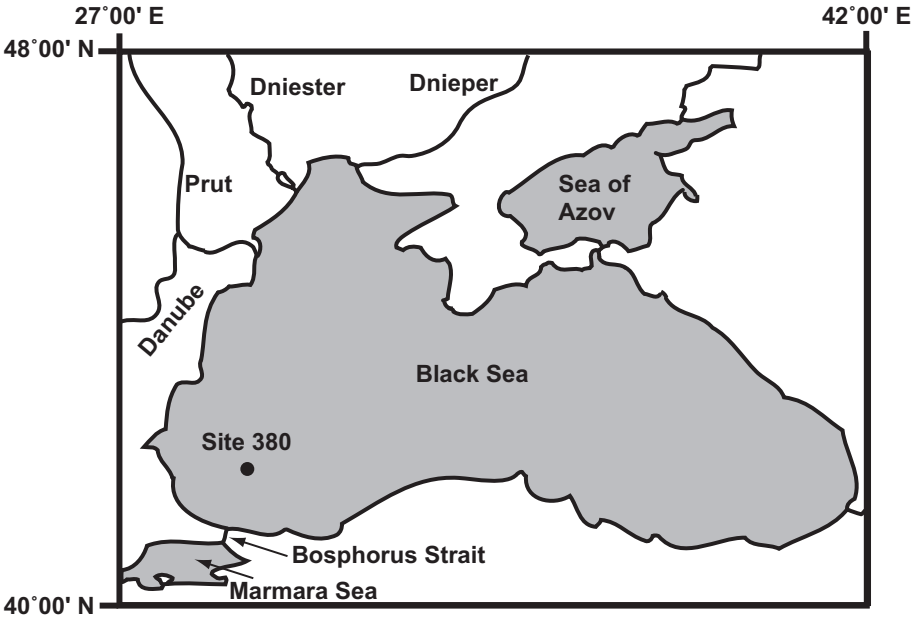

Fig. 2. Map of the Black Sea, with the location of DSDP Leg 42B, Site 380.

inifera and ostracods were determined at the generic level for general paleo-environmental assessment. Shell preservation was determined to evaluate if the shells were reworked.

2.5. Inorganic carbon and oxygen isotopes

Measurements of $\delta^{13}C_{carb}$ and $\delta^{18}O$ on benthic foraminiferal and ostracod tests were made using a Micromass Optima mass spectrometer with an attached Multiprep peripheral for the automated analysis of carbonates. An in-house standard, calibrated against NBS-19, was used to adjust the stable isotope values to V-SMOW using 1.95‰ and −2.16‰ for $\delta^{13}C_{carb}$ and $\delta^{18}O$, respectively (Coplen et al., 1983; Coplen, 1995). The standard deviations ($1-\sigma$) of the standards analyzed during the sample runs were 0.05‰ and 0.08‰ for $\delta^{13}C_{carb}$ and $\delta^{18}O$, respectively.

2.6. Trace element analyses

The method for sediment digestion for major and trace elements followed the digestion protocol of Franzese (2008). Approximately 25–30 mg of bulk powdered sediment was dissolved in a mix of 4 mL of 8 N HNO_3 (Fisher Scientific, Optima Grade) and 250 μL concentrated HF (Fisher Scientific, Optima Grade) and heated for 3 h at ~200 °C. The samples were then taken to dryness, reacted at 150 °C with 1 mL of aqua regia (1:3 HNO_3:HCl) to remove organic material. Following removal of the aqua regia, a second addition of 8 N HNO_3/250 μL HF solution was added and the samples were sonicated for 20–30 min and heated again to complete dissolution. Samples were taken to dryness, and then heated with 500 μL HNO_3 to remove any fluorides created by the digestion process. Samples were finally dissolved in 700 μL of 3% HNO_3.

Samples were measured for major elements Fe, Mn, Al, Ca, and Ti with an Inductively Coupled Plasma Optical Emission Spectrometer (ICP-OES, Vista Pro, Varian Inc., Australia). The instrumental analyses were performed using the instrumental parameters described in Quan et al. (2008), using a CETAC Technologies ASX-500 autosampler (CETAC Technologies Inc., Omaha, NE). Trace elements (Mo, Re, and U) were measured using a High Resolution Inductively Coupled Plasma Mass Spectrometer (HR-ICP-MS, Element-1, ThermoFinnegan, Bremen, Germany) as detailed in Quan et al. (2008). Final concentrations, calculated after normalization to internal standards, pseudo-standard addition and procedural blank subtraction as described in Cullen et al. (2001) exhibit better than ±5% precision and accuracy. Concentrations were also adjusted for $CaCO_3$ content by assuming all Ca was present as $CaCO_3$; concentrations are reported on a $CaCO_3$-free basis. Detection limits for the ICP-OES were 7 ppm for Al, 5 ppm for Ca, 2 ppm for Fe, 0.3 ppm for Ti, and 0.05 ppm for Mn; HR-ICP-MS detection limits were 2.0 ppb for Mo, 0.007 ppb for Re, and 0.12 ppb for U.

2.7. Statistical analyses

To characterize and identify statistical differences in the data, we performed analysis of variance (ANOVA Type III) (PROC GLM; SAS Institute; SAS v. 9.3) with depth class as a fixed effect and the various geochemical data elements as the response variables. Depth classes used were 0.89–11.35 mbsf, 12.85–41.72 mbsf, 43.36–67.23 mbsf, and 76.74–118.31 mbsf. In instances where significant variance with depth was determined, we performed Tukey's multiple comparison tests to determine which depth classes differed significantly from one another for the element under analysis (Zar, 1999).

3. RESULTS

3.1. Lithostratigraphy and micropaleontology

Shipboard lithostratigraphy on Leg 42 divides the upper 145 m of Site 380 into five lithostratigraphic subunits (Ross, 1978). Subunit Ia was not recovered at Site 380, but was designated as a subunit with a lithology equivalent to Holocene aged nannofossil oozes reported in several Black Sea cores. Subunit Ib is a sapropel based on the organic rich muds found in the highly disturbed, upper 2 m of Site 380. This lithology is correlative to other sapropels found in the Black Sea. Subunit Ic extends from 2 mbsf down to 42 mbsf and is described as muds with sandy silts. Freshwater diatoms are found in this subunit, indicating deposition in freshwater conditions. The lithology of Subunit Id is a diatomaceous mud and is noted for its very strong marine influence, based on the microfossil groups (diatom, nannofossils and planktonic foraminifera) found within this zone. This subunit extends from 42 to 76 mbsf. The fifth subunit (Ie) encompasses 76–145 mbsf and is described as lacustrine sediments with a rare occurrences of brackish water diatoms.

Our micropaleontological analyses are consistent with the shipboard subdivisions, but shed additional light on the paleo-environmental assignments. Based on the combined shipboard observations (Ross, 1978) and those in this study, we subdivide the upper 120 m of Site 380 into four intervals (Table 1 and Fig. 3). Interval 1 spans the upper 12 m of Site 380 and is based on the presence of the freshwater ostracod *Candona* and absence of other ostracod taxa with brackish affinities. We have only one sample in the upper 2 m and see no evidence in our assemblage data to warrant a subdivision at 2 mbsf as suggested in the Leg 42 report. Our interval 2 extends from 12 to 41.5 mbsf based on the co-occurrence of *Candona* and brackish ostracod taxa *Leptocythere* and *Bacunella* (Olteanu, 1978). The co-occurrence of both brackish and freshwater taxa indicates either stratified water column or seasonally varying salinities. The base of our interval 2 is 50 cm higher than that Subunit Ic identified in the shipboard lithostratigraphic report and must reflect differences in how the hydraulic connection to the Mediterranean manifests itself in lithology vs the response of the micropaleontologic communities to this change. Benthic foraminifera (*Anomalinoides, Elphidium, Discorbis*, *and Nonion* spp.) characterized as brackish to marine species (Kaiho, 1991, 1994; Kaminski et al., 2002) were found in both intervals 1 and 2.

Our interval 3 is defined as the interval containing samples in which planktonic foraminifera are found (41.5–76.8 mbsf). This interval is equivalent to lithostratigraphic subunit Id in the Site 380 report (Ross, 1978). Planktonic foraminiferal specimens are juveniles with translucent tests and likely carried in from a Mediterranean connection. The drastic change in water conditions in the Black Sea most likely resulted in the death of all planktonic foraminifera. Adult tests quickly sank, whereas the more buoyant juvenile forms were carried much further in the Black Sea before sinking. A few samples in interval 3 also contained benthic foraminifera. Interval 4 ranges from 76.8 to 118.31 mbsf and is barren of microfossils.

3.2. Nitrogen and carbon data

The downcore record of $\delta^{15}N$ values from Black Sea core 380 ranges from +3.1‰ to +5.9‰, and tracks the four lithological intervals (ANOVA $P < 0.001$; Table 1; Fig. 3). Samples from the uppermost interval 1 (0.89–11.35 mbsf) have relatively low $\delta^{15}N$ values, ranging from 4.0‰ to 4.9‰, averaging 4.4 ± 0.3‰ (SD). Isotopically enriched $\delta^{15}N$ values characterize samples from interval 2 (12.85–41.72 mbsf), which average 5.4 ± 0.4‰, and range from 5.0‰ to 5.9‰. In the third interval (43.36–67.23 mbsf), measured $\delta^{15}N$ values average $\delta^{15}N = 3.6 \pm 0.3$‰ and range from 3.1‰ to 4.0‰, slightly lower than those obtained in interval 1. Interval 4 (76.74–118.31 mbsf) records $\delta^{15}N$ values similar to those from interval 2, averaging 5.3 ± 0.4‰ and ranging from 4.7‰ to 5.9‰ (Tukey $P > 0.05$). Downcore $\delta^{13}C_{org}$ values range from −29.0‰ to −23.6‰, but the data for individual intervals are not drastically different statistically (ANOVA $P = 0.04$; Tukey $P > 0.05$), with average $\delta^{13}C_{org}$ values within each interval close to the overall profile average (-25.6 ± 1).

Total nitrogen (%TN) ranges from 0.03% to 0.24% (Table 1; Fig. 3). Intervals 2, and 4 generally have similar %TN values (0.12 ± 0.02%, and 0.10 ± 0.02%, respectively), while %TN values for intervals 1 (0.06 ± 0.03%) and 3 (0.17 ± 0.03%) are statistically different (Tukey $P < 0.05$). Percent total organic carbon (%TOC) ranges from 0.2% to 1.6%; interval 3 has over twice the amount of TOC (1.2 ± 0.2%; Tukey $P < 0.05$) than intervals 1, 2, and 4 (0.4 ± 0.1%, 0.6 ± 0.1% and 0.5 ± 0.2%, respectively). The higher %TN and %TOC values for interval 3 are likely due to anoxic conditions preventing oxidation of the sedimentary organic matter. These TOC values are very similar to those reported in the Leg 42 initial reports (Emelyanov, et al., 1978). C/N ratios range from 3.4 to 8.7 (mol/mol), with an average of 6 ± 1.

3.3. Redox-sensitive metals

Profiles for Al, Ti, Fe, Mn, Mo, U, and Re are shown in Fig. 4 with values listed in Table 2. All redox-sensitive metals are divided by Al concentrations to eliminate the effect of varying input sources. The data for Al and Ti indicate that the detrital input to the Black Sea at this location, while variable, do not show consistent trends through the core. The profiles for Mo, and Re indicate a significant increase in metal concentration in interval 3 compared to intervals 1, 2, and 4 (Tukey $P < 0.05$), though the enrichment is not consistent across the whole interval. The U, Fe, and Mn profiles do not indicate any statistically significant enrichment in any one interval, but interval 3 values are slightly higher on average. Mo, U, and Re also exhibit a distinct decrease in concentration at 51.2 mbsf (interval 3) but concentrations generally recover quickly.

3.4. Ostracod and foraminifera ^{18}O measurements

We performed genus-level $\delta^{18}O$ measurements for *Candona* spp. (freshwater ostracod), *Leptocythere* spp. and *Bacunella* spp. (brackish-water ostracods), and *Anomalinoides* spp. (benthic foraminifera) (Table 1 and

Table 1
Isotopic and bulk elemental measurements for the Black Sea samples.

Depth (mbsf)	$\delta^{15}N$‰	%TN	$\delta^{13}C_{org}$‰	%TOC	C/N	Planktonic foraminifera	*Candona* spp. ($\delta^{18}O$‰)	Benthic foraminifera ($\delta^{18}O$‰)	Ostracods: *Bacunella* and *Leptocythere* spp. ($\delta^{18}O$‰)
0.89	4.7	0.08	−24.2	0.51	6.4	N	N	N	N
2.39	4.0	0.04	−24.7	0.34	8.4	N	N	Y (−2.2‰ [a])	N
3.33	4.3	0.06	−24.7	0.39	6.5	N	N	N	N
6.81	4.7	0.09	−26.2	0.51	5.7	N	Y (−6.9‰)	N	N
7.94	4.9	0.09	−25.5	0.52	5.8	N	Y	N	N
10.65	4.2	0.03	−24.2	0.26	8.7	N	Y	Y (−1.9‰ [a])	N
11.35	4.2	0.03	−23.6	0.18	6.1	N	Y (−7.2‰)	N	N
12.85	5.6	0.08	−26.0	0.46	5.7	N	Y	Y (−0.2‰ [a])	N
28.89	5.8	0.13	−24.3	0.55	4.2	N	N	Y (−1.1‰ [a])	Y (−5.2‰ [b])
30.80	5.1	0.12	−24.5	0.57	4.8	N	Y (−7.9‰)	N	N
31.93	5.8	0.13	−24.2	0.68	5.2	N	N	Y	Y (−3.8‰ [c])
33.63	5.0	0.13	−24.5	0.81	6.2	N	N	Y (−0.8‰ [a])	N
39.00	5.9	0.10	−26.8	0.56	5.6	N	Y (−5.5‰)	Y (−0.5‰ [a])	Y (−5.5 ± 0.3‰ [b], −5.3‰ [c])
40.57	5.1	0.11	−26.2	0.51	4.6	N	Y (−8.1‰)	Y (−1 ± 1‰ [a])	Y (−5.1 ± 0.9‰ [b], −4.9‰ [c])
41.72	5.0	0.13	−26.1	0.64	4.9	Y	N	Y	N
43.36	4.0	0.24	−26.6	1.42	5.9	N	N	N	N
48.25	4.0	0.18	−26.2	1.28	7.0	N	N	N	N
50.30	3.7	0.15	−26.1	0.96	6.4	Y	N	N	N
51.22	3.4	0.15	−26.8	1.06	7.1	Y	N	Y (−0.2‰ [a])	Y (−6.4‰ [b])
52.81	3.7	0.18	−25.1	1.17	6.5	Y	N	Y	N
58.34	3.2	0.12	−25.3	0.88	7.3	N	N	N	N
58.78	3.5	0.18	−26.4	1.28	7.1	Y	N	Y	N
61.23	3.4	0.15	−26.0	1.03	6.9	N	N	N	N
61.68	3.7	0.18	−26.0	1.19	6.6	Y	N	N	N
67.23	3.1	0.20	−25.4	1.55	7.8	Y	N	N	N
76.74	4.7	0.08	−25.5	0.41	5.1	Y	Y (−4.8‰)	N	N
76.98	5.9	0.09	−27.3	0.46	5.1	N	N	N	N
85.90	5.7	0.10	−26.9	0.34	3.4	N	N	N	N
86.80	5.2	0.07	−25.3	0.36	5.1	N	N	N	N
88.10	4.9	0.09	−25.3	0.48	5.3	N	N	N	N
91.07	5.5	0.10	−25.4	0.37	3.7	N	N	N	N
96.32	5.1	0.12	−29.0	1.03	8.4	N	N	N	N
114.21	5.5	0.09	−25.3	0.39	4.3	N	N	N	N
118.31	5.7	0.12	−24.9	0.41	3.4	N	N	N	N

[a] *Anomalinoides* spp.
[b] *Bacunella* spp.
[c] *Leptocythere* spp.

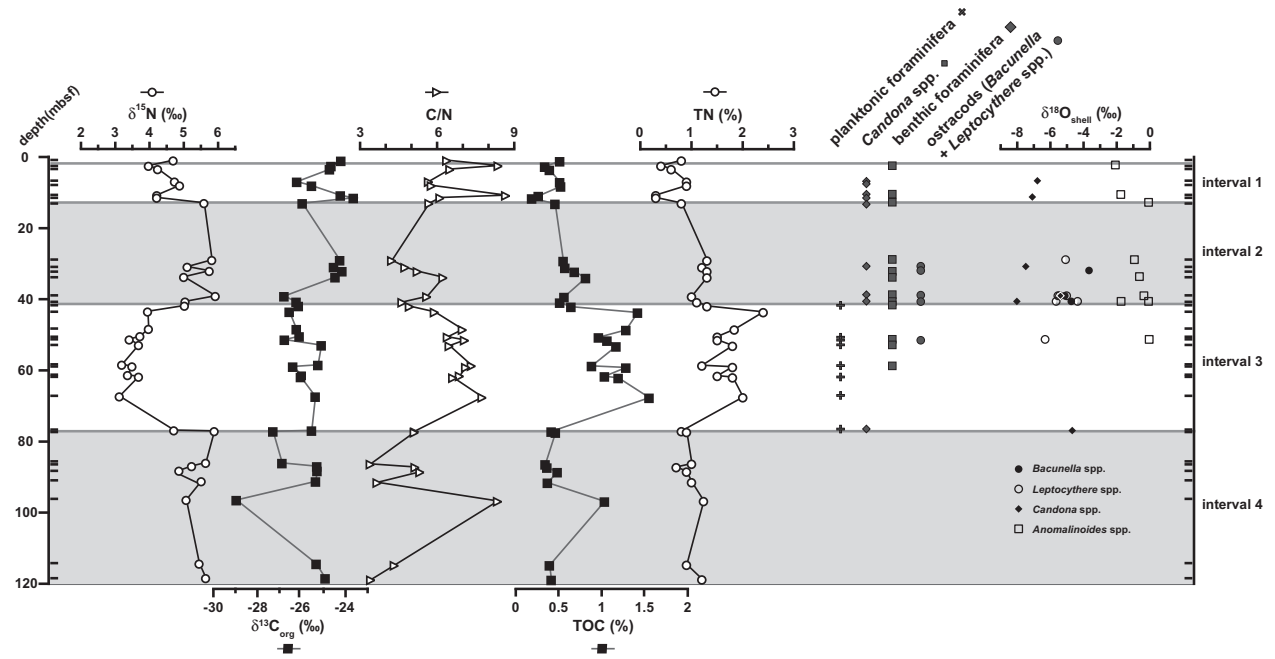

Fig. 3. Isotopic and elemental profiles for Black Sea DSDP 42B Hole 380. Intervals marked indicate shifts in $\delta^{15}N$ corresponding to changes in the redox state of the deep water column.

Fig. 3). Isotopic values for *Candona* spp. range from $-8.1‰$ to $-4.8‰$, with an average value of $-7 \pm 1‰$ ($n = 6$). All but one of these values are from intervals 1 and 2; the "$-4.8‰$" value is from a sample at the boundary between intervals 3 and 4. The $\delta^{18}O$ values for brackish-water ostracod genera *Leptocythere* spp. and *Bacunella* spp. are $-5.3‰$ to $-3.8‰$ (average -4.6 ± 0.8, $n = 3$) and $-6.4‰$ to $-4.5‰$ (average -5.5 ± 0.6, $n = 7$), respectively. *Anomalinoides* spp. $\delta^{18}O$ values range from $-2.2‰$ to $-0.2‰$, with an average of $-1.0 \pm 0.8‰$ ($n = 9$). Planktonic foraminifera were too rare and small for oxygen isotope analysis.

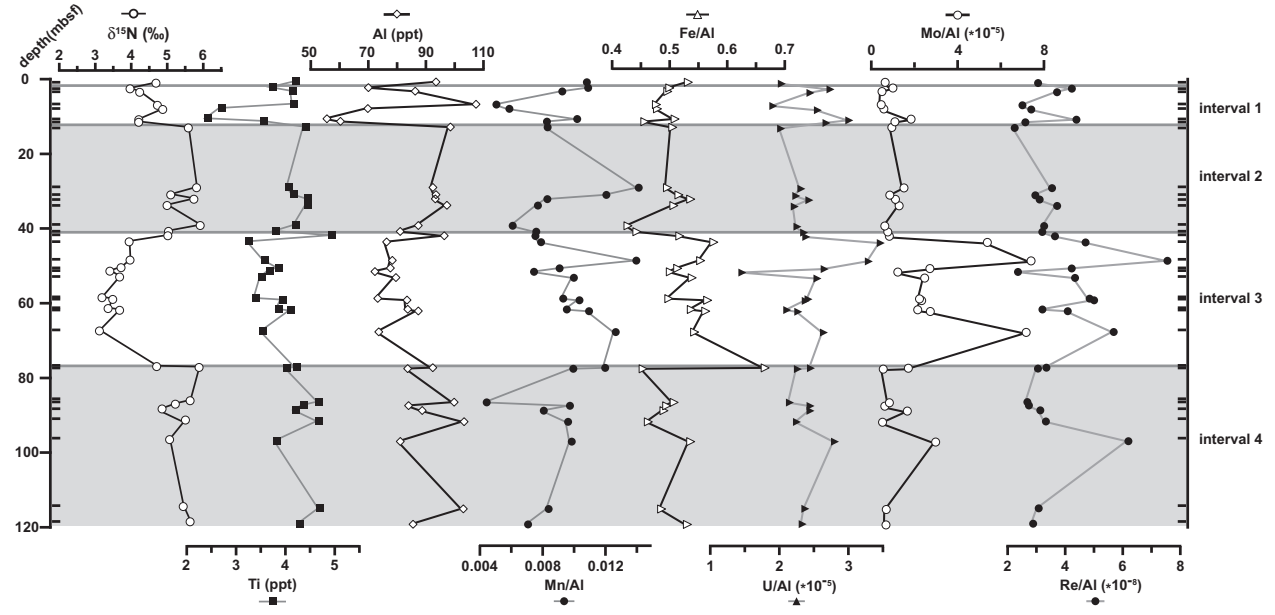

Fig. 4. Al, Ti, Mn, Fe profiles from Black Sea DSDP Leg 42B, Hole 380. Intervals marked in gray correspond to the changes in $\delta^{15}N$ profile.

Table 2
Elemental concentrations for Al, Ti, Fe, Mn, Mo, U, Re and Ca in whole rock samples.

Depth (mbsf)	Al (ppt)	Fe (ppt)	Mn (ppt)	Ti (ppt)	Mo (ppm)	U (ppm)	Re (ppb)	Ca (ppt)
0.89	92.6	48.9	0.99	4.16	0.51	1.86	2.8	67.8
2.39	69.1	34.3	0.74	3.69	0.63	1.88	2.9	65.0
3.33	85.4	42.0	0.78	4.09	0.35	2.07	3.1	53.3
6.81	106.5	50.3	0.52	4.13	0.39	2.01	2.6	38.4
7.94	68.9	32.7	0.39	2.65	0.34	1.74	1.9	27.3
10.65	54.7	27.6	0.55	2.37	0.96	1.63	2.4	122.9
11.35	59.4	26.9	0.48	3.52	0.60	1.58	1.5	72.5
12.85	97.6	48.9	0.80	4.36	0.84	1.95	2.1	37.8
28.89	91.6	45.0	1.28	4.02	1.30	2.10	3.2	28.1
30.80	92.6	47.4	1.10	4.13	0.71	2.05	2.7	39.8
31.93	92.4	49.2	0.75	4.40	0.95	2.22	2.8	33.9
33.63	96.4	48.5	0.73	4.40	1.16	2.12	3.5	44.2
39.00	86.5	36.6	0.51	4.16	0.46	1.93	2.8	51.7
40.57	80.2	35.2	0.60	3.76	0.54	1.87	2.5	42.5
41.72	95.5	49.0	0.70	4.90	0.71	2.26	3.4	34.3
43.36	75.5	43.2	0.58	3.22	3.99	2.60	3.5	17.4
48.25	77.5	42.6	1.07	3.54	5.66	2.53	5.8	44.0
50.30	76.8	39.1	0.68	3.82	2.02	2.02	3.2	39.8
51.22	71.4	35.5	0.52	3.63	0.81	1.03	1.6	37.9
52.81	78.7	42.1	0.77	3.48	1.88	1.99	3.4	55.0
58.34	72.4	35.8	0.66	3.35	1.55	1.73	3.5	57.2
58.78	82.6	46.4	0.84	3.90	1.85	1.94	4.1	35.9
61.23	82.8	44.2	0.78	3.81	1.71	1.73	2.6	42.7
61.68	86.5	48.3	0.93	4.07	2.29	1.94	3.5	41.1
67.23	72.7	39.2	0.91	3.49	5.15	1.90	4.1	44.2
76.74	91.5	60.5	1.08	4.18	1.49	2.22	3.0	53.3
76.98	82.8	37.2	0.81	3.99	0.38	1.85	2.5	39.0
85.90	83.1	40.8	0.80	4.34	0.44	2.01	2.2	25.5
86.80	98.9	49.8	0.42	4.64	0.74	2.10	2.6	50.1
88.10	87.8	42.7	0.69	4.16	1.39	2.13	2.7	37.6
91.07	102.4	46.9	0.97	4.63	0.44	2.28	3.3	51.1
96.32	80.2	42.7	0.78	3.77	2.32	2.23	4.9	37.0
114.21	102.1	49.2	0.84	4.66	0.62	2.40	3.1	60.2
118.31	84.7	44.6	0.58	4.24	0.50	1.96	2.4	26.4

Concentrations for Al, Ti, Fe, Mn, Mo, U, and Re were corrected for $CaCO_3$ dilution effects by assuming all measured Ca was in carbonate form, then recalculating elemental concentrations using the $CaCO_3$-free sample mass.

4. DISCUSSION

4.1. Nitrogen isotopes

Our results reveal a clear pattern of variation in $\delta^{15}N$ composition in the sediments of the Black Sea indicating that nitrogen cycling in the basin changed drastically on millennial time scales (Fig. 3). Intervals 1 and 3 are characterized by depleted $\delta^{15}N$ values, similar to modern-day Black Sea sediments (~2.5‰ to 3.6‰; Fry et al., 1991; Çoban-Yıldız et al., 2006). Intervals 2 and 4 have distinctly enriched $\delta^{15}N$ values, indicating increased fractionation due to denitrification relative to intervals 1 and 3. Based on the model outlined in Quan et al. (2008), the fractionation due to water column denitrification is maximized under suboxic conditions, indicating that intervals 2 and 4 were deposited during periods when suboxia was relatively extensive. Such conditions were transiently established when the Black Sea transitioned from oxic, freshwater conditions to anoxic marine conditions or vice versa. This suggests that either interval 1 or interval 3 was deposited during an oxic, freshwater period, where water column oxygen levels were too high for significant amounts of denitrification. The remaining interval would represent an anoxic depositional environment similar to the modern-day Black Sea, where either water column oxygen levels are too low to support significant amounts of nitrate, or denitrification goes to completion, or nitrogen fixation is elevated due to significant loss of nitrogen via denitrification (Haug et al., 1998; Fulton et al., 2012). Both depositional environments would be characterized by lower nitrogen isotope values. Based on the $\delta^{15}N$ data and the theoretical $\delta^{15}N$ vs. O_2 model, we hypothesize that interval 1 represents an oxic redox condition likely resulting from the isolated Black Sea lake, while interval 3 was deposited in an anoxic environment similar to the modern day Black Sea.

4.2. Assigning redox stratigraphy

Although the nitrogen isotope measurements clearly record dramatic changes in the Black Sea over the sampling interval, it is critical to connect these changes to variations in redox state. The simplest approach would be to use dating and stratigraphy to determine glacial and interglacial

intervals; however, there is no consensus chronostratigraphy for Site 380. Several different indices were used in the initial reports and later by Schrader (1979), but in combination they are problematic, and, in some cases, contradictory (see Schrader (1979) for a complete discussion of these issues). Most of the indices support placing the Eemian between 50 and 100 mbsf, followed by the Weichselian from 0–50 mbsf, with no recovery of Holocene. This chronology requires that estimated sedimentation rates range from approximately 80–100 cm/kyr during the sampled interval, though the presence of turbidites have undoubtedly resulted in higher estimated sedimentation rates (Schrader, 1979). While these sedimentation rates are higher than those calculated from other Black Sea cores, they are still of similar order of magnitude (Jørgensen et al., 2004; Popescu et al., 2010). The chronology outlined in Schrader (1979) supports our general findings; however, the identification of specific glacial–interglacial $\delta^{18}O$ isotope stages is less important to our hypothesis than determining water column redox state. It is also possible that weaker glacials may not sever the connection between the Black Sea and the Mediterranean completely, and thus are not recorded in the geochemical proxies we have analyzed, or that a decline in sea level during interglacials could be reflected in the proxies. Another consideration is that tectonic activity may have altered the depth of the Bosphorus and/or route to the Black Sea (Nazik et al., 2011 and references within).

The TN and TOC profiles support our assignments of particular intervals as oxic/anoxic/suboxic. While it is possible that changes in organic matter content are related to changes in the relative amount of terrestrial organic matter input, the lack of correlation between TOC and $\delta^{13}C_{org}$, and TN and $\delta^{13}C_{org}$ does not support that hypothesis. In addition, a TN versus TOC regression (Calvert, 2004; Knies et al., 2007) indicates that the amount of inorganic nitrogen input is statistically the same for oxic (interval 1), anoxic (interval 3), and suboxic (intervals 2 and 4) environments (98% confidence interval, Student's *t*-test) and that the fraction of inorganic nitrogen in the samples is effectively zero (see Supplementary Fig. S1).

An independent measure of sedimentary redox is based on the concentrations of redox sensitive elements (Fe, Mn, Mo, U, and Re) relative to authigenic non-transition metals, Al and Ti. Both Al and Ti content decreased slightly through interval 3, which likely corresponds to a small degree of dilution of the terrestrial input from the rivers with marine sources while the Black Sea was connected to the Mediterranean Sea, but statistical analysis indicates that this interval is not statistically unique (not all interval 3 Tukey analyses have $P < 0.05$), indicating that the riverine (detrital) input to the Black Sea has remained generally consistent over this period of time (Fig. 4). The Fe/Al ratio, a reliable paleoredox proxy (Lyons and Severmann, 2006), reveals a slight enrichment during interval 3 relative to the rest of the core, which is attributed to pyrite deposition under euxinic conditions. Unfortunately, the Site 380 samples were suspected to have undergone post-coring re-oxidation soon after the initial recovery (Berner and Holdren, 1978), so measurements of different species of Fe, which would potentially be indicative of redox conditions and deep water oxygen conditions (i.e. pyritic Fe and acid-soluble Fe for degree of pyritization calculations; see Raiswell et al. (1988)) could not be performed, though pyrite was found by the initial reports in this part of the core (Schrader, 1978). However, the three trace metals in this study (U, Re, and Mo), form a gradient with respect of ease of enrichment under reducing conditions. Uranium is the earliest along the diagenetic sequence, and can be enriched under suboxic, anoxic, and euxinic conditions as reduced U(IV) species are less soluble; U enrichment in sediments is also correlated to high TOC content (Algeo and Maynard, 2004; Tribovillard et al., 2006). Rhenium enrichment can also occur under suboxic, anoxic, and euxinic conditions as the soluble Re oxyanion is reduced to a less soluble species (Ravizza et al., 1991; Colodner et al., 1993; Crusius et al., 1996), but there is evidence that the Re enrichment peak occurs deeper in sedimentary columns than the U maximum as U undergoes reduction first (Crusius et al., 1996). Unlike U and Re, Mo geochemistry indicates that it is enriched under sulfidic (euxinic) conditions, but not under suboxic or anoxic conditions as high dissolved sulfide levels are necessary to form insoluble thiomolybdate species (Crusius et al., 1996; Helz et al., 1996; Algeo and Maynard, 2004; Algeo and Lyons, 2006; Tribovillard et al., 2006). As a result of differences, we can use the combination of these three elements to determine the redox differences in the sediments between the intervals outlined in the $\delta^{15}N$ record.

All three metal/Al ratios are enriched in interval 3 compared to intervals 1, 2 and 4, supporting our hypothesis that the sediments in interval 3 were deposited in an euxinic period (Fig. 4). U/Al and Re/Al also indicate slight enrichments in interval 1, but based on the $\delta^{15}N$ data and the micropaleontology (discussed in the next section), this enrichment is probably not due to anoxia during deposition. It is more likely that the U and Re peaks are due to post-depositional processes; there is also some evidence that U and Re concentrations in sediments may not be entirely dictated by thermodynamics and thus may not be able to reliably distinguish between oxic and suboxic conditions (Nameroff et al., 2002). We are also limited by our lack of knowledge of the dynamics and circulation patterns of the lacustrine Black Sea. The metal concentrations for all three metals throughout the measured sections are at least 10 times lower than published values for the Black Sea, though the pattern of enrichment in anoxic intervals compared to oxic periods remains the same (Ravizza et al., 1991; Crusius et al., 1996; Lüschen, 2004; Nagler et al., 2005; Algeo and Lyons, 2006). However, the published measurements were not made on the same core or time interval as our data, and the few Mo/Al measurements reported in the initial reports are very similar to our values; therefore we conclude that the lower concentrations are characteristic of this site (Emelyanov et al., 1978). While it should be noted that these redox metal measurements may only be accurate proxies of the sediment redox conditions, they can still provide insights into the redox state of the water column.

There appears to be a period (61.7–50.3 mbsf) in the middle of interval 3 where the Mo concentration dropped precipitously, and remained low for several meters. Based

on Mo geochemistry, the depositional environment during this period was either no longer sulfidic enough for Mo scavenging, or was too sulfidic, leading to depletion of the aqueous Mo reservoir, and therefore less Mo burial (Algeo and Lyons, 2006). This change may reflect redox instability in the water column during this interval, resulting in a brief oxygenation of the sediments and a decrease in Mo deposition. This instability may be due to a reduction in the marine inflow to the Black Sea through the Bosphorus Strait (Waelbroeck et al., 2002). This may also explain why there is only one main U peak in interval 3; the second was lost due to remobilization upon reoxygenation of the sediments. The Re profile also indicates evidence of post-depositional remobilization since the deeper peak is less intense than the higher one (Crusius et al., 1996; Tribovillard et al., 2006). There is also no evidence that the enrichments in interval 3 are due to the presence of turbidites, as measured Al and Ti concentrations are very similar to the other three intervals. We were also unable to visually detect any turbidite layers in our samples.

Micropaleontological and lithological analysis further supports the identification of interval 1 as a freshwater period and interval 3 as deposited under marine conditions. The shipboard lithostratigraphy divides our research section into intervals that are consistent with those set by our geochemical and micropaleontological analyses, as discussed in Section 3.1. The presence of the freshwater ostracod *Candona* and absence of any marine planktonic foraminifera indicate freshwater conditions associated with deposition during interval 1 (Table 1, Fig. 3). Ostracods are frequently used as paleoenvironmental proxies, and *Candona* have been used in the Black Sea to evaluate predominantly freshwater periods (Olteanu, 1978; Bahr et al., 2006, 2008). Ostracod genera *Leptocythere* and *Bacunella* are characteristic of brackish water environments (Olteanu, 1978). These genera are found only at base of interval 2, which supports our hypothesis that that interval is a transitional one, and a single sample at the boundary of intervals 3 and 4, during the period the metal profiles suggest a suboxic/oxic hiatus in the interglacial. The average $\delta^{18}O_{shell}$ values for the *Candona* samples from intervals 1 and 2 are $-7 \pm 1‰$, reflecting growing conditions primarily dominated by riverine input (Özsoy et al., 2002; Bahr et al., 2006). The *Candona* sample from the boundary between intervals 3 and 4 is more enriched in ^{18}O, possibly indicating slightly more marine input in the basin. Oxygen isotope measurements for *Bacunella* spp. and *Leptocythere* spp. shells exhibit little variation, suggesting that their water column salinity did not change significantly between late interval 3 and early interval 2.

Only samples from interval 3 contained juvenile planktonic foraminifera tests. (Table 1, Fig. 3). Since planktonic foraminifera are exclusively marine, we deduce that the water column in interval 3 was primarily marine, and, by analogy to modern conditions, also stratified and anoxic due to the connection to the Mediterranean Sea. The planktonic foraminifera found were all juvenile forms, so identification of specific genera present and oxygen isotope analysis were not possible. It is likely that these organisms were carried into the Black Sea via flow from the Mediterranean and Marmara Seas but were unable to grow in the less saline surface waters in the Black Sea and sank to the sediments. Adult planktonic foraminifera probably died and sank long before the currents carried them to Site 380. Only one of the studied samples contained both planktonic foraminifera and the freshwater *Candona*; this sample lies at the base of interval 3, indicating that the tests and shells that were found were predominantly mutually exclusive except at the transitional point from freshwater to marine conditions.

We were able to identify four different brackish to suboxic genera from the Black Sea samples: *Anomalinoides*, *Elphidium*, *Discorbis*, and *Nonion* spp. (Gheorghian, 1978; Kaiho, 1991, 1994; Kaminski et al., 2002) (Table 1, Fig. 3). These genera were present all through interval 1, which is expected given our interpretation that this interval represents an oxic, lacustrine environment. The majority of the samples in interval 2 also contained benthic foraminifera supporting the geochemical evidence that interval 2 was a brackish transitional period between marine (interval 3) and freshwater (interval 1) endmembers, and that the sediment-water interface must have had some minimal amount of oxygen (estimated < 1.5 mL/L; Kaiho, 1994) present on occasion in order to support these organisms. This assignment is supported by the fact that the interval 3 samples that contain these benthic foraminifera are within the suboxic/oxic hiatus indicated by the trace metal profiles. The $\delta^{18}O_{shell}$ values for *Anomalinoides* spp. tests were statistically similar throughout the three intervals, regardless of environmental conditions. Assuming that the vital effect for *Anomalinoides* spp. remains the same through this period of time, it would appear that the $\delta^{18}O$ value of the benthic water layer remained consistent through this period despite changes in oxidation state, even though the $\delta^{18}O$ of the water should scale with salinity (Rank et al., 1999; Aksu et al., 2002). The lack of micropaleontological specimens in interval 4 prevents us from evaluating the environmental conditions in this interval based on biotic preferences; however, comparison of geochemical data with that of interval 2 implies similar suboxic conditions. Although micropaleontology cannot directly prove whether the water column was oxic, suboxic, or anoxic, the determination of freshwater versus marine combined with the geochemical evidence and geological history of the Black Sea provides strong inference supporting our assignments of water column redox state.

4.3. The Paleo-nitrogen cycle of the Black Sea

Based on our data and published information, we have reconstructed the Black Sea paleoenvironmental conditions that occurred during our sampled sediment core section. Fig. 5 compares both the theoretical relationship of sedimentary $\delta^{15}N$ and water column O_2 levels for our hypothesized redox scenario (Fig. 5A), and the actual measured $\delta^{15}N$ profile (Fig. 5B). The deepest section (interval 4) is a suboxic period characterized by brackish waters with low oxygen concentrations, higher $\delta^{15}N$ values (average $5.3 \pm 0.4‰$), and relatively high amounts of denitrification. It is likely that this period represents a transition between

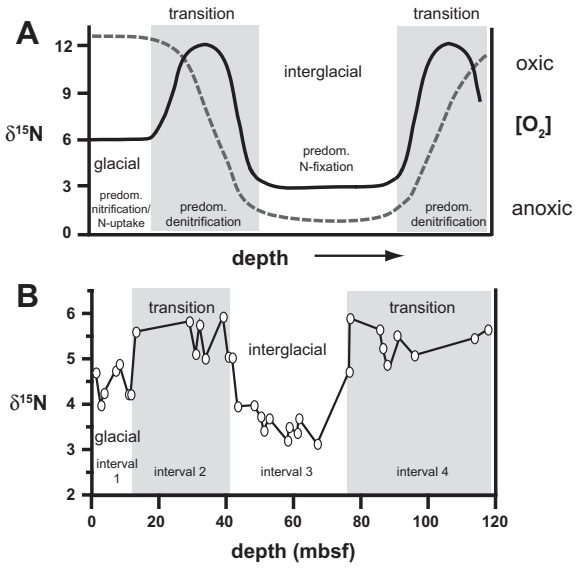

Fig. 5. Part A indicates the predicted $\delta^{15}N$ profile (solid line) as determined using the conceptual model in Quan et al. (2008) applied to the redox changes (dashed line) in the sampled section of DSDP Site 380. Predominant nitrogen reactions that control the $\delta^{15}N$ values produced through time are also indicated. This predicted $\delta^{15}N$ record is very similar to the actual measured profile in part B, confirming our hypothesis.

the lacustrine (oxic) and marine-influenced (anoxic) end-members, recording the influx of anoxic marine water through the Bosphorus into the then-oxic Black Sea. The designation of interval 4 is perhaps the most tenuous, as we were unable to isolate any micropaleontological evidence from this interval; however, similarities in the geochemical proxies between interval 4 and interval 2, and the hypothesized glacial–interglacial cycling patterns of the Black Sea provide support for this assignment.

Interval 3 represents fully anoxic, marine conditions that may have been periodically unstable, as supported by enriched levels of redox-sensitive trace metals, higher TOC and TN concentrations, and depleted $\delta^{15}N$ values (average $3.6 \pm 0.3‰$). This evidence for strongly marine-influenced, anoxic conditions similar to the modern-day Black Sea implies that interval 3 likely represents an interglacial period (perhaps Marine Isotope Chron 5e), where the Black Sea basin is fully connected to the Mediterranean; $\delta^{15}N$ values in interval 3 are very similar to sedimentary $\delta^{15}N$ values measured in the deep basin of the present-day Black Sea (Fry et al., 1991; Çoban-Yıldız et al., 2006; Fuchsman et al., 2008) and samples through Black Sea Unit I (modern interglacial) (Fulton et al., 2012).

The lower $\delta^{15}N$ values in interval 3 may also be due to increased nitrogen fixation in the Black Sea in response to the loss of nitrogen via increased productivity and an intense amount of denitrification, similar to the explanation of Haug et al. (1998) for lower $\delta^{15}N$ values during interglacial conditions in the Cariaco Basin. Evidence of nitrogen fixation has been identified in the Black Sea, but the intensity and consistency of the process, and thus the effect it has on the $\delta^{15}N$ signal on millennial time scales, is unknown (McCarthy et al., 2007; Fuchsman et al., 2008; Fulton et al., 2012). However, this alternate explanation for the lower $\delta^{15}N$ values in interval 3 does not contradict our conclusion that the Black Sea was a stratified, anoxic, marine-influenced basin during this interval.

Interval 2 represents a suboxic, brackish water period. Increasing oxygen levels compared to interval 3 are implied due to higher $\delta^{15}N$ values (average $5.4 \pm 0.4‰$) as well as the presence of brackish water benthic foraminifera and ostracod genera. While the geochemistry is similar to interval 4, interval 2 likely represents the opposite process: the transitional period between the anoxic interglacial and oxic glacial as the decrease in sea level cuts off marine input from the Mediterranean Sea.

Interval 1 sediments were deposited under oxic water column conditions when the Black Sea was an oxic, freshwater or brackish lake, dominated by nitrate assimilation and buffered by atmospheric nitrogen, as inferred by average $\delta^{15}N$ values of $4.4 \pm 0.3‰$, lower concentrations of redox-sensitive metals in the deposited sediments, and the presence of ostracods and benthic foraminifera. This interval likely represents the last glacial period, perhaps the low sea level stand of isotope stage 2. According to the initial reports, the first sample at 0.89 mbsf is the only sample that might represent post-glacial conditions, as sediments from the present-day sapropel and transition into the last glacial were not recovered in this core; our data seem to indicate this sample could also have been deposited during an oxic period with the rest of interval 1. This overall sequence of events (intervals 4 through 1) as depicted by Fig. 5, is driven by redox changes in the Black Sea bottom waters, and matches well with our hypothesized schematic in Fig. 1.

For the majority of the samples, we are able to confirm our hypothesis that the measured $\delta^{15}N$ record can be correlated to the redox state of the Black Sea at the time of deposition. The apparent exception to this is the zone between 50–60 mbsf (interval 3), characterized by a period of lower redox-sensitive metal concentrations in the otherwise enriched interval. We also find benthic foraminifera during the same period, though the bottom waters during interval 3 would likely be sulfidic. This period of apparent (sub)oxygenation is not reflected in the $\delta^{15}N$ record, even though the model predicts that $\delta^{15}N$ values should increase as oxygen levels rise. There is evidence that the interglacial represented by interval 3 was unstable and may have been punctuated by at least 2 colder climate phases (Koroneva and Kartashova, 1978), which may have resulted in the lowering of sea levels by 20–30 m (Waelbroeck et al., 2002). This would reduce the depth of the water in the Bosphorus Strait, resulting in limited marine input to the Black Sea, lack of deeper outflow from the basin, and altered circulation patterns within the Black Sea.

Why does the relationship between $\delta^{15}N$ and redox state break down during this period? Unfortunately, not enough is known about the Pleistocene Black Sea circulation, water depth, and nutrient utilization to give a definitive answer. From our data, it appears that $\delta^{15}N$, $\delta^{13}C_{org}$, $\delta^{13}C_{inorg}$, TOC, C/N, and TN are unaffected, so there was likely no major overturning of the Black Sea to fully oxic levels, no

obvious disruption of the carbon cycle, and the volume of the suboxic zone (and thus the relative amount of denitrification compared to other N processes) must have remained approximately the same. We hypothesize that lowered sea level reduced the amount of marine input and increased the relative strength of the CIL, increasing the oxygenation of the lateral intrusions into the deep sea. In the current interglacial Black Sea, these lateral oxygenated intrusions can be seen to a water depth of 500–700 m and over 200 km into the Black Sea basin (Özsoy et al., 1991; Konovalov et al., 2003); the DSDP Site 380 is within that 200 km range, though the current water depth is much deeper. If the sea level in the basin was lower, and the CIL relatively stronger, it is possible that these intrusions could penetrate to the sediments. These intrusions would not dramatically change the redox state of the Black Sea water layers on a basin-wide scale, but may have a significant impact on specific locations. As a result, the net nitrogen cycle does not significantly change, but the slight oxygenation at this location might have inhibited the trace metal enrichment, particularly of those requiring sulfidic conditions.

It is possible that the shifts seen in the nitrogen isotope record may simply result from changes in the $\delta^{15}N$ of inorganic nutrients as the marine input to the Black Sea waxes and wanes relative to the riverine input. Unfortunately, we do not have a good estimate of the nitrogen concentrations or $\delta^{15}N$ values of riverine and marine waters during this period, though it can probably be assumed that they would be significantly different from the anthropogenically-altered modern Black Sea. Nitrogen isotope values for DOM in relatively unpolluted Arctic rivers (Amon and Meon, 2004; Talbot, 2001) suggest that a relative increase in pre-anthropogenic freshwater input would probably lower the $\delta^{15}N$ values in the Black Sea, which could explain the more depleted values in both intervals 1 and 3; however, our redox-sensitive metal and micropaleontological data contradict a predominantly freshwater system in interval 3. We also do not see geologically significant shifts in $\delta^{13}C_{org}$ or C/N occurring in concert with the changes in measured bulk $\delta^{15}N$, as would be expected if a shift in the organic matter source was the driving force behind the $\delta^{15}N$ record. Finally, we also do not see significant changes in the fraction of detrital inorganic N to the Black Sea (Supplementary Fig. S1).

Variations in sedimentary $\delta^{15}N$ over time can occur in the absence of source $\delta^{15}N$ changes if the redox state of the environment drives corresponding changes in the local nitrogen cycle. For example, variations in the size of oxygen-deficient zones, and therefore variations in the relative intensity of denitrification in these zones, are recorded in sediment records in the Eastern North Pacific, Mexican coastal margin, and the Arabian Sea; these redox variations are driven by reduced oxidant demand rather than a change in nitrogen source (Ganeshram et al., 1995, 2000, 2002). Similarly, variations in $\delta^{15}N$ in glacial–interglacial records of the Cariaco Basin are seen even though the $\delta^{15}N$ of the nitrate of the source waters was likely relatively constant (Haug et al., 1998). While there is not enough information about the deposition and circulation patterns in the paleo-Black Sea and the surrounding areas to completely eliminate a change in $\delta^{15}N$ input as the root cause of the measured $\delta^{15}N$ profile, we suggest that the changes in $\delta^{15}N$, redox-sensitive metals, and micropalontology can be simply explained by variations in water column redox conditions.

5. CONCLUSIONS

This study reports the first record of sedimentary $\delta^{15}N$ measured for a deep sea core from the Black Sea on a glacial–interglacial time scale. We were able to correlate the sedimentary $\delta^{15}N$ record with changes in the deep water redox state in the Black Sea water column in response to glacial–interglacial conditions. The $\delta^{15}N$ record also indicates that the Black Sea nitrogen cycle has changed significantly through time in response to glacial–interglacial redox changes, and provides a starting point for further research into paleo-nutrient cycling in the basin. These results thus provide qualitative support for our conceptual model relating long-term changes in sedimentary nitrogen isotopes to redox state in the overlying waters.

ACKNOWLEDGEMENTS

Support for this research was provided by the Agouron Institute and the NASA Exobiology Program. T. M. Quan was also supported by the IMCS Postdoctoral Fellowship program. We thank Drs. Steven Calvert and Silke Severmann and three anonymous reviewers for their helpful comments on this manuscript. Drs. Janette Steets and Mark Payton provided advice on the statistical analyses.

APPENDIX A. SUPPLEMENTARY DATA

Supplementary data associated with this article can be found, in the online version, at http://dx.doi.org/10.1016/j.gca.2013.02.029.

REFERENCES

Aksu A. E., Hiscott R. N. and Yasar D. (1999) Oscillating quaternary water levels of the Marmara Sea and vigorous outflow into the Aegean Sea from the Marmara Sea–Black Sea drainage corridor. *Mar. Geol.* **153**, 275–302.

Aksu A. E., Hiscott R. N., Kaminski M. A., Mudie P. J., Gillespie H., Abrajano T. and Yaşar D. (2002) Last glacial-Holocene paleoceanography of the Black Sea and Marmara Sea: stable isotopic, foraminiferal, and coccolith evidence. *Mar. Geol.* **190**, 119–149.

Algeo T. J. and Lyons T. W. (2006) Mo-total organic carbon covariation in modern anoxic marine environments: implications for analysis of paleoredox and paleohydrographic conditions. *Paleoceanography* **21**. http://dx.doi.org/10.1029/2004PA001112.

Algeo T. J. and Maynard J. B. (2004) Trace-element behavior and redox facies in core shales of Upper Pennsylvanian Kansas-type cyclothems. *Chem. Geol.* **206**, 289–318.

Altabet M. A. and Francois R. (1994) Sedimentary nitrogen isotopic ratio as a recorder for surface ocean nitrate utilization. *Global Biogeochem. Cycles* **8**, 103–116.

Amon R. M. W. and Meon B. (2004) The biogeochemistry of dissolved organic matter and nutrients in two large Arctic

estuaries and potential implications for our understanding of the Arctic Ocean system. *Mar. Chem.* **92**, 311–330.

Arnold G. L., Anbar A. D., Barling J. and Lyons T. W. (2004) Molybdenum isotope evidence for widespread anoxia in mid-Proterozoic oceans. *Science* **304**, 87–90.

Bahr A., Arz H. W., Lamy F. and Wefer G. (2006) Late glacial to Holocene paleoenvironmental evolution of the Black Sea, reconstructed with stable oxygen isotope records obtained on ostrocod shells. *Earth Planet. Sci. Lett.* **241**, 863–875.

Bahr A., Lamy F., Arz H. W., Major C., Kwiecien O. and Wefer G. (2008) Abrupt changes of temperature and water chemistry in the late Pleistocene and early Holocene Black Sea. *Geochem. Geophys. Geosyst.* **9**, Q01004. http://dx.doi.org/10.1029/2007GC001683.

Berner R. A. and Holdren, Jr., G. R. (1978) Sulfur distribution in Holes 380 and 380A of Leg 42B. In *Initial Report of the Deep Sea Drilling Project* (eds. D. A. Ross and Y. P. Neprochnov, et al.). U.S. Government Printing Office, Washington, pp. 625–626.

Calvert S. E. (2004) Beware intercepts: interpreting compositional ratios in multi-component sediments and sedimentary rocks. *Org. Geochem.* **35**, 981–987.

Calvert S. E., Vogel J. S. and Southon J. R. (1987) Carbon accumulation rates and the origin of the Holocene sapropel in the Black Sea. *Geology* **15**, 918–921.

Calvert S. E., Pedersen T. F. and Karlin R. E. (2001) Geochemical and isotopic evidence for post-glacial palaeoceanographic changes in Saanich Inlet, British Columbia. *Mar. Geol.* **174**, 278–305.

Çoban-Yıldız Y., Altabet M. A., Yılmaz A. and Tuğrul S. (2006) Carbon and nitrogen isotopic ratios of suspended particulate organic matter (SPOM) in the Black Sea water column. *Deep-Sea Res. II* **53**, 1875–1892.

Codispoti L. A., Friederich G. E., Murray J. W. and Sakamoto C. M. (1991) Chemical variability in the Black Sea: implications of continuous vertical profiles that penetrated the oxic/anoxic interface. *Deep Sea Res. Part A* **38**, S691–S710.

Colodner D., Sachs J., Ravizza G., Turekian K., Edmond J. and Boyle E. (1993) The geochemical cycle of rhenium: a reconnaissance. *Earth Planet. Sci. Lett.* **117**, 205–221.

Coplen T. B. (1995) Reporting of stable carbon, hydrogen and oxygen isotopic abundances. In *Reference and Intercomparison Materials for Stable Isotopes of Light Elements* (ed. IAEA-TECDOC). IAEA, Vienna, pp. 31–34.

Coplen T. B., Kendall C. and Hopple J. (1983) Intercomparison of stable isotope reference samples. *Nature* **203**, 236–238.

Cowie G. L., Mowbray S., Lewis M., Matheson H. and McKenzie R. (2009) Carbon and nitrogen elemental and stable isotopic compositions of surficial sediments from the Pakistan margin of the Arabian Sea. *Deep Sea Res. II* **56**, 271–282.

Crusius J., Calvert S., Pedersen T. and Sage D. (1996) Rhenium and molybdenum enrichments in sediments as indicators of oxic, suboxic and sulfidic conditions of deposition. *Earth Planet. Sci. Lett.* **145**, 65–78.

Cullen J. T., Field M. P. and Sherrell R. M. (2001) Determination of trace elements in filtered suspended marine particulate material by sector field HR-ICP-MS. *J. Anal. Atom. Spectrom.* **16**, 1307–1312.

Dumitrescu M. and Brassell S. C. (2006) Compositional and isotopic characteristics of organic matter for the early Aptian Oceanic Anoxic Event at Shatsky Rise, ODP Leg 198. *Palaeogeogr. Palaeoclimatol. Palaeoecol.* **235**, 168–191.

Emelyanov E. M., Lisitzen A. P., Shimkus K. M., Trimonis E. S., Lukashev V. K., Liukashin V. N., Mitropolskiy A. Y. and Pilipchik M. F. (1978) Geochemistry of Late Cenozoic sediments of the Black Sea, Leg 42B. In *Initial Report of the Deep Sea Drilling Project* (eds. D. A. Ross and Y. P. Neprochnov, et al.). U.S. Government Printing Office, Washington, pp. 543–605.

Emmer E. and Thunell R. C. (2000) Nitrogen isotope variations in Santa Barbara Basin sediments: implications for denitrification in the eastern tropical North Pacific during the last 50,000 years. *Paleoceanography* **15**, 377–387.

Falkowski P. G. (1997) Evolution of the nitrogen cycle and its influence on the biological sequestration of CO_2 in the ocean. *Nature* **387**, 272–275.

Falkowski P. G. and Godfrey L. V. (2008) Electrons, life and the evolution of Earth's oxygen cycle. *Philos. Trans. R. Soc. London, B* **363**. http://dx.doi.org/10.1098/rstb.2008.0054.

Fennel K., Follows M. and Falkowski P. G. (2005) The co-evolution of the nitrogen, carbon and oxygen cycles in the Proterozoic ocean. *Am. J. Sci.* **305**, 526–545.

Franzese A. M. (2008) Paleoceanography of the Agulhas Current and Retroflection determined by radiogenic isotopes in sediments. Ph. D. thesis, Columbia University.

Fry B., Jannasch H. W., Molyneaux S. J., Wirsen C. O., Muramoto J. A. and King S. (1991) Stable isotope studies of the carbon, nitrogen and sulfur cycles in the Black Sea and the Cariaco Trench. *Deep-Sea Res.* **38**, S1003–S1019.

Fuchsman C. A., Murray J. W. and Konovalov S. K. (2008) Concentration and natural stable isotope profiles of nitrogen species in the Black Sea. *Mar. Chem.* **111**, 90–105.

Fulton J. M., Arthur M. A. and Freeman K. H. (2012) Black Sea nitrogen cycling and the preservation of phytoplankton $\delta^{15}N$ signals during the Holocene. *Global Biogeochem. Cycles* **26**, GB2030. http://dx.doi.org/10.1029/2011gb004196.

Ganeshram R. S., Pedersen T. F., Calvert S. E. and Murray J. W. (1995) Large changes in oceanic nutrient inventories from glacial to interglacial periods. *Nature* **376**, 755–758.

Ganeshram R. S., Pedersen T. F., Calvert S. E., McNeill G. W. and Fontugne M. R. (2000) Glacial–interglacial variability in denitrification in the world's oceans: causes and consequences. *Paleoceanography* **15**, 361–376.

Ganeshram R. S., Pedersen T. F., Calvert S. E. and François R. (2002) Reduced nitrogen fixation in the glacial ocean inferred from changes in marine nitrogen and phosphorus inventories. *Nature* **415**, 156–159.

Gaye-Haake B., Lahajnar N., Emeis K.-C., Unger D., Rixen T., Suthhof A., Ramaswamy V., Schulz H., Paropkari A. L., Guptha M. V. S. and Ittekkot V. (2005) Stable nitrogen isotopic ratios of sinking particles and sediments from the northern Indian Ocean. *Mar. Chem.* **96**, 243–255.

Gheorghian M. (1974) Distribution pattern of benthonic foraminifera on continental shelf of Black Sea off Rumanian shore. In *The Black Sea-Geology, Chemistry, and Biology* (eds. E. T. Degens and D. A. Ross). The American Association of Petroleum Geologists, Tulsa, Oklahoma, pp. 411–418.

Gheorghian M. (1978) Micropaleontological investigations of sediments from Sites 379, 380, and 381 of Leg 42B. In *Initial Report of the Deep Sea Drilling Project* (eds. D. A. Ross and Y. P. Neprochnov, et al.). U.S. Government Printing Office, Washington, pp. 783–787.

Gregg M. C. and Yakushev E. (2005) Surface ventilation of the Black Sea's cold intermediate layer in the middle of the western gyre. *Geophys. Res. Lett* **32**, L03604. http://dx.doi.org/10.1029/02004GL021580.

Haug G. H., Pedersen T. F., Sigman D. M., Calvert S. E., Nielsen B. and Peterson L. C. (1998) Glacial/interglacial variations in production and nitrogen fixation in the Cariaco Basin during the last 580 kyr. *Paleoceanography* **13**, 427–432.

Helz G. R., Miller C. V., Charnock J. M., Mosselmans J. F. W., Pattrick R. A. D., Garner C. D. and Vaughan D. J. (1996)

Mechanism of molybdenum removal from the sea and its concentration in black shales: EXAFS evidence. *Geochim. Cosmochim. Acta* **60**, 3631–3642.

Hsü K. J. (1978a) Stratigraphy of the lacustrine sedimentation in the Black Sea. In *Initial Report of the Deep Sea Drilling Project* (eds. D. A. Ross and Y. P. Neprochnov, et al.). U.S. Government Printing Office, Washington, pp. 509–524.

Hsü K. J. (1978b) Correlation of Black Sea sequences. In *Initial Report of the Deep Sea Drilling Project* (eds. D. A. Ross and Y. P. Neprochnov, et al.). U.S. Government Printing Office, Washington, pp. 489–497.

Jenkyns H. C., Gröcke D. R. and Hesselbo S. P. (2001) Nitrogen isotopic evidence for water mass denitrification during the early Toarcian (Jurassic) oceanic anoxic event. *Paleoceanography* **16**, 593–603.

Jenkyns H. C., Jones C. E., Gröcke D. R., Hesselbo S. P. and Parkinson D. N. (2002) Chemostratigraphy of the Jurassic System: applications, limitations and implications for palaeoceanography. *J. Geol. Soc. London* **159**, 351–378.

Jenkyns H. C., Matthews A., Tsikos H. and Erel Y. (2007) Nitrate reduction, sulfate reduction, and sedimentary iron isotope evolution during the Cenomanian-Turonian oceanic anoxic event. *Paleoceanography* **22**, PA3208. http://dx.doi.org/10.1029/2006PA001355.

Jørgensen B. B., Böttcher M. E., Lüschen H., Neretin L. N. and Volkov I. I. (2004) Anaerobic methane oxidation and a deep H_2S sink generate isotopically heavy sulfides in Black Sea sediments. *Geochim. Cosmochim. Acta* **68**, 2095–2118.

Juniam C. K. and Arthur M. A. (2007) Nitrogen cycling during the Cretaceous, Cenomanian-Turonian Oceanic anoxic event II. *Geochem. Geophys. Geosyst.* **8**, Q03002. http://dx.doi.org/10.1029/2006GC001328.

Kaiho K. (1991) Global changes of Paleogene aerobic/anaerobic benthic foraminifera and deep-sea circulation. *Palaeogeogr. Palaeoclimatol. Palaeoecol.* **83**, 65–85.

Kaiho K. (1994) Benthic foraminiferal dissolved-oxygen index and dissolved-oxygen levels in the modern ocean. *Geology* **22**, 719–722.

Kaminski M. A., Aksu A., Box M., Hiscott R. N., Filipescu S. and Al-Salameen M. (2002) Late Glacial to Holocene benthic foraminifera in the Marmara Sea: implications for Black Sea–Mediterranean Sea connections following the last deglaciation. *Mar. Geol.* **190**, 165–202.

Kienast S. S., Calvert S. E. and Pedersen T. F. (2002) Nitrogen isotope and productivity variations along the northeast Pacific margin over the last 120 kyr: surface and subsurface paleoceanography. *Paleoceanography* **17**, PA1055. http://dx.doi.org/10.1029/2001PA000650.

Knies J., Brookes S. and Schubert C. J. (2007) Re-assessing the nitrogen signal in continental margin sediments: new insights from the high northern latitudes. *Earth Planet. Sci. Lett.* **253**, 471–484.

Konovalov S. K., Luther, III, G. W., Friedrich G. E., Nuzzio D. B., Tebo B. M., Murray J. W., Oguz T., Glazer B., Trouwborst R. E., Clement B., Murray K. J. and Romanov A. S. (2003) Lateral injection of oxygen with the Bosphorus plume-fingers of oxidizing potential in the Black Sea. *Limnol. Ocean.* **48**, 2369–2376.

Konovalov S. K., Murray J. W. and Luther, III, G. W. (2005) Basic processes of Black Sea biogeochemistry. *Oceanography* **18**, 24–35.

Koroneva E. V. and Kartashova G. G. (1978) Palynological study of samples from Holes 379A, 380A, Leg 42B. In *Initial Report of the Deep Sea Drilling Project* (eds. D. A. Ross and Y. P. Neprochnov, et al.). U.S. Government Printing Office, Washington, pp. 951–992.

Kuypers M. M. M., Sliekers A. O., Lavik G., Schmid M., Jorgensen B. B., Kuenen J. G., Damste J. S. S., Strous M. and Jetten M. S. M. (2003) Anaerobic ammonium oxidation by anammox bacteria in the Black Sea. *Nature* **422**, 608–611.

Kwiecien O., Arz H. W., Lamy F., Wulf S., Bahr A., Röhl U. and Haug G. H. (2008) Estimated reservoir ages of the Black Sea since the last glacial. *Radiocarbon* **50**, 99–118.

Lüschen H. (2004) Vergleichende anorganisch-geochemische Untersuchungen an phanerozoischen Corg-reichen Sedimenten: Eiin Beitrag zur Charakterisierung ihrer Fazies. Ph. D. thesis, Carl von Ossietzky Universität Oldenburg.

Lyons T. W. (1991) Upper Holocene sediments of the Black Sea: summary of Leg 4 box cores (1988 Black Sea oceanographic expedition). In *Black Sea Oceanography* (eds. E. Izdar and J. W. Murray). Springer, New York, pp. 401–441.

Lyons T. W. and Severmann S. (2006) A critical look at iron paleoredox proxies based on new insights from modern euxinic marine basins. *Geochim. Cosmochim. Acta* **70**, 5698–5722.

Major C., Ryan W., Lericolais G. and Hajdas I. (2002) Constraints on Black Sea outflow to the Sea of Marmara during the last glacial–interglacial transition. *Mar. Geol.* **190**, 19–34.

Major C. O., Goldstein S. L., Ryan W. B. F., Lericolais G., Piotrowski A. M. and Hajdas I. (2006) The co-evolution of Black Sea level and composition through the last deglaciation and its paleoclimatic significance. *Quaternary Sci. Rev.* **25**, 2031–2047.

McCarthy J. J., Yilmaz A., Coban-Yildiz Y. and Nevins J. L. (2007) Nitrogen cycling in the offshore waters of the Black Sea. *Estuar. Coast. Shelf Sci.* **74**, 493–514.

Moore J. K. and Doney S. C. (2007) Iron availability limits the ocean nitrogen inventory stabilizing feedbacks between marine denitrification and nitrogen fixation. *Global Biogeochem. Cycles* **21**, GB2001. http://dx.doi.org/10.1029/2006GB002762.

Murray J. W., Top Z. and Özsoy E. (1991) Hydrographic properties and ventilation of the Black Sea. *Deep Sea Res. II* **38**, 663–689.

Murray J. W., Codispoti L. A. and Friederich G. E. (1995) Oxidation–reduction environments: the suboxic zone in the Black Sea. In *Aquatic Chemistry: Interfacial and Interspecies Processes* (eds. C. P. Huang, C. R. O'Melia and J. J. Morgan). American Chemical Society, Washington, DC, pp. 157–176.

Murray J. W., Fuchsman C., Kirkpatrick J., Paul B. and Konovalov S. K. (2005) Species and $\delta^{15}N$ signatures of nitrogen transformations in the suboxic zone of the Black Sea. *Oceanography* **18**, 36–47.

Nagler T. F., Siebert C., Lüschen H. and Böttcher M. E. (2005) Sedimentary Mo isotope record across the Holocene fresh–brackish water transition of the Black Sea. *Chem. Geol.* **219**, 283–295.

Nameroff T. J., Balistrieri L. S. and Murray J. W. (2002) Suboxic trace metal geochemistry in the Eastern Tropical North Pacific. *Geochim. Cosmochim. Acta* **66**, 1139–1158.

Naqvi S. W. A., Naik H., Pratihary A., D'Souza W., Narvekar P. V., Jayakumar D. A., Devol A. H., Yoshinari T. and Saino T. (2006) Coastal versus open-ocean denitrification in the Arabian Sea. *Biogeosciences* **3**, 621–633.

Nazik A., Meriç E., Avsar N., Ünlü S., Esenli V. and Gökaşan E. (2011) Possible waterways between the Marmara Sea and the Black Sea in the late Quaternary: evidence from ostracod and foraminifer assemblages in lakes İznik and Sapanca, Turkey. *Geo-Mar. Lett.* **31**, 75–86.

Neretin L. N., Böttcher M. E., Jørgensen B. B., Volkov I. I., Lüschen H. and Hilgenfeldt K. (2004) Pyritization processes and greigite formation in the advancing sulfidization front in the upper Pleistocene sediments of the Black Sea. *Geochim. Cosmochim. Acta* **68**, 2081–2093.

Olteanu R. (1978) Ostracoda from DSDP Leg 42B. In *Initial Report of the Deep Sea Drilling Project* (eds. D. A. Ross and Y. P. Neprochnov, et al.). U.S. Government Publishing Office, Washington, pp. 1017–1038.

Özsoy E., Top Z., White G. and Murray J. W. (1991) Double diffusive intrusions, mixing and deep convection processes in the Black Sea. In *Black Sea Oceanography* (eds. E. Izdar and J. W. Murray). Springer, London, pp. 17–42.

Özsoy E., Rank D. and Salihoglu I. (2002) Pycnocline and deep mixing in the Black Sea: stable isotope and transient tracer measurements. *Estuar. Coast. Shelf Sci.* **54**, 621–629.

Popescu S.-M. (2006) Late Miocene and early Pliocene environments in the southwestern Black Sea region from high-resolution palynology of DSDP Site 380A (Leg 42B). *Palaeogeogr. Palaeoclimatol. Palaeoecol.* **238**, 64–77.

Popescu S.-M., Biltekin D., Winter H., Suc J.-P., Melinte-Dobrinescu M. C., Klotz S., Rabineau M., Combourieu-Nebout N., Clauzon G. and Deaconu F. (2010) Pliocene and Lower Pleistocene vegetation and climate changes at the European scale: long pollen records and climatostratigraphy. *Quatern. Int.* **219**, 152–167.

Pride C., Thunell R., Sigman D., Keigwin L., Altabet M. and Tappa E. (1999) Nitrogen isotopic variations in the Gulf of California since the last deglaciation: response to global climate change. *Paleoceanography* **14**, 397–409.

Quan T. M. and Falkowski P. G. (2009) Redox control of N:P ratios in aquatic ecosystems. *Geobiology* **7**, 124–139.

Quan T. M., van de Schootbrugge B., Field M. P., Rosenthal Y. and Falkowski P. G. (2008) Nitrogen isotope and trace metal analyses from the Mingolsheim core (Germany): evidence for redox variations across the Triassic–Jurassic boundary. *Global Biogeochem. Cycles* **22**, GB2014. http://dx.doi.org/10.1029/2007GB002981.

Raiswell R., Buckley F., Berner R. A. and Anderson T. F. (1988) Degree of pyritization of iron as a paleoenvironmental indicator of bottom-water oxygenation. *J. Sed. Petrol.* **58**, 812–819.

Rank D., Özsoy E. and Salihoğlu I. (1999) Oxygen-18, deuterium and tritium in the Black Sea and the Sea of Marmara. *J. Environ. Radioactivity* **43**, 231–245.

Ravizza G., Turekian K. K. and Hay B. J. (1991) The geochemistry of rhenium and osmium in recent sediments from the Black Sea. *Geochim. Cosmochim. Acta* **55**, 3741–3752.

Ross D. A. (1978) Summary of results of Black Sea drilling. In *Initial Report of the Deep Sea Drilling Project* (eds. D. A. Ross and Y. P. Neprochnov, et al.). U.S. Government Printing Office, Washington, pp. 1149–1178.

Ross D. A. and Degens E. T. (1974) Recent sediments of Black Sea. In *The Black Sea-Geology, Chemistry, and Biology* (eds. E. T. Degens and D. A. Ross). The American Association of Petroleum Geologists, Tulsa, OK, p. 633.

Ryabenko E., Kock A., Bange H. W., Altabet M. A. and Wallace D. W. R. (2012) Contrasting biogeochemistry of nitrogen in the Atlantic and Pacific Oxygen Minimum Zones. *Biogeosciences* **9**, 203–215.

Ryan W. B. F., Pitman, III, W. C., Major C. O., Shimkus K., Moskalenko V., Jones G., Dimitrov P., Gorur N., Sakinc M. and Yuce H. (1997) An abrupt drowning of the Black Sea shelf. *Mar. Geol.* **138**, 119–126.

Ryan W. B. F., Major C. O., Lericolais G. and Goldstein S. L. (2003) Catastrophic flooding of the Black Sea. *Ann. Rev. Earth Planet. Sci.* **31**, 525–554.

Schrader H.-J. (1978) Quaternary through Neogene history of the Black Sea, deduced from the paleoecology of diatoms, silicoflagellates, Ebridians, and Chrysomonads. In *Initial Report of the Deep Sea Drilling Project* (eds. D. A. Ross and Y. P. Neprochnov, et al.). U.S. Government Printing Office, Washington, pp. 798–901.

Schrader H. J. (1979) Quaternary paleoclimatology of the Black Sea basin. *Sed. Geol.* **23**, 165–180.

Sigman D. M., DiFiore P. J., Hain M. P., Deutsch C. and Karl D. M. (2009) Sinking organic matter spreads the nitrogen isotopic signal of pelagic denitrification in the North Pacific. *Geophys. Res. Lett.* **36**, L08605. http://dx.doi.org/10.1029/2008GL035784.

Talbot M. R. (2001) Nitrogen isotopes in paleolimnology. In *Tracking Environmental Change Using Lake Sediments Volume 2: Physical and Geochemical Methods* (eds. W. M. Last and J. P. Smol). Kluwer Academic Publishers, Dordrecht, The Netherlands, pp. 401–439.

Thunell R. C. and Kepple A. B. (2004) Glacial-Holocene $\delta^{15}N$ record from the Gulf of Tehuantepec, Mexico: implication for denitrification in the eastern equatorial Pacific and changes in atmospheric N_2O. *Global Biogeochem. Cycles* **18**, GB1001. http://dx.doi.org/10.1029/2002GB002028.

Thunell R. C., Sigman D. M., Muller-Karger F., Astor Y. and Varela R. (2004) Nitrogen isotope dynamics of the Cariaco Basin, Venezuela. *Global Biogeochem. Cycles* **18**, GB3001. http://dx.doi.org/10.1029/2003GB002185.

Traverse A. (1978) Palynological analysis of DSDP Leg 42B (1975) cores from the Black Sea. In *Initial Report of the Deep Sea Drilling Project* (eds. D. A. Ross and Y. P. Neprochnov, et al.). U.S. Government Publishing Office, Washington, pp. 993–1015.

Tribovillard N., Algeo T. J., Lyons T. W. and Riboulleau A. (2006) Trace metal as paleoredox and paleoproductivity proxies: an update. *Chem. Geol.* **232**, 12–32.

Waelbroeck C., Labeyrie L., Michel E., Duplessy J. C., McManus J. F., Lambeck K., Balbon E. and Labracherie M. (2002) Sea-level and deep water temperature changes derived from benthic foraminifera isotopic records. *Quaternary Sci. Rev.* **21**, 295–305.

Ward B. B., Devol A. H., Rich J. J., Chang B. X., Bulow S. E., Naik H., Pratihary A. and Jayakumar A. (2009) Denitrification as the dominant nitrogen loss process in the Arabian Sea. *Nature* **461**, 78–81.

Yanko-Hombach V. (2007) Controversy over Noah's Flood in the Black Sea: geological and foraminiferal evidence from the shelf. In *The Black Sea Flood Question: Changes in Coastline, Climate, and Human Settlement* (eds. V. Yanko-Hombach and A. S. Gilbert, et al.). Springer, Dordrecht, The Netherlands, pp. 149–203.

Zar J. H. (1999) *Biostatistical Analysis*, 4th ed. Prentice Hall, Upper Saddle River, New Jersey, USA.

Associate editor: Timothy Lyons